

Multiaccuracy and Multicalibration via Proxy Groups

Beepul Bharti^{1,2}
bbharti1@jhu.edu

Mary Versa Clemens-Sewall³
mcleme18@jhu.edu

Paul H. Yi⁴
paul.yi@stjude.org

Jeremias Sulam^{1,2,5}
jsulam1@jhu.edu

¹Mathematical Institute for Data Science (MINDS), Johns Hopkins University

²Department of Biomedical Engineering, Johns Hopkins University

³Department of Applied Mathematics & Statistics, Johns Hopkins University

⁴St. Jude Children's Research Hospital

⁵Department of Computer Science, Johns Hopkins University

March 5, 2025

Abstract

As the use of predictive machine learning algorithms increases in high-stakes decision-making, it is imperative that these algorithms are fair across sensitive groups. Unfortunately, measuring and enforcing fairness in real-world applications can be challenging due to missing or incomplete sensitive group data. Proxy-sensitive attributes have been proposed as a practical and effective solution in these settings, but only for parity-based fairness notions. Knowing how to evaluate and control for fairness with missing sensitive group data for newer and more flexible frameworks, such as multiaccuracy and multicalibration, remains unexplored. In this work, we address this gap by demonstrating that in the absence of sensitive group data, proxy-sensitive attributes can provably be used to derive actionable upper bounds on the true multiaccuracy and multicalibration, providing insights into a model's potential worst-case fairness violations. Additionally, we show that adjusting models to satisfy multiaccuracy and multicalibration across proxy-sensitive attributes can significantly mitigate these violations for the true, but unknown, sensitive groups. Through several experiments on real-world datasets, we illustrate that approximate multiaccuracy and multicalibration can be achieved even when sensitive group information is incomplete or unavailable.

Contents

1	Introduction	3
1.1	Related Work	4
1.2	Our Contributions	5
2	Setting and Background	5
3	Multiaccuracy and Multicalibration	6
4	Bounds on Multigroup Fairness Violations	7
5	Reducing Worst-Case Violations	8
6	Experimental Results	10
6.1	ACS Experiments	10
6.1.1	ACSIncome	11
6.1.2	ACSPublicCoverage (ACSPubCov)	11
6.2	CheXpert	12
7	Conclusion	13
A	Additional Theoretical Results	18
B	Proofs	18
B.1	Proof of Lemma 4.1	18
B.2	Proof of Theorem 4.2	19
B.3	Proof of Theorem 5.1	19
C	Additional Experiment Details	20
C.1	ACS Experiments	20
C.2	CheXpert	20
D	Additional Tables	21
E	Additional Figures	22

1 Introduction

Predictive machine learning algorithms are increasingly used in high-stakes decision-making contexts such as healthcare [SSJ18], employment [FC21], credit scoring [TCE17], and criminal justice [RWC20]. Although these models demonstrate impressive overall performance, growing evidence indicates that they often exhibit biases and discriminate against certain sensitive groups [OM19; Das22]. For instance, ProPublica’s investigation [Ang+22] revealed significant racial disparities in recidivism risk assessment algorithms, which disproportionately classified African Americans as high-risk for re-offending. As the deployment of these algorithms increases, regulatory bodies worldwide, including the US Office of Science and Technology Policy (OSTP) [SP22], European Union [Com21], and United Nations [UU21], have emphasized the importance of ensuring that predictive algorithms avoid discrimination and uphold fairness.

These concerns have led to the emergence of *algorithmic fairness*, a field dedicated to ensuring that predictive models do not inadvertently discriminate against sensitive groups defined by attributes such as race, age, or biological sex. Unfortunately, measuring and controlling a model’s fairness can be challenging in many real-world settings, as sensitive group data is often incomplete or unavailable [Hol+19; GPS+23]. In certain contexts, like healthcare, privacy and legal regulations such as the HIPAA Privacy Rule restrict access to sensitive data. In other cases, the information was not collected because it was considered unnecessary [WH11; Fre+16; Zha18]. Despite these obstacles, it remains crucial to evaluate a model’s fairness before and during its deployment. This raises the question: how can we evaluate and promote fairness when sensitive group information is imperfect or missing altogether?

One popular approach, widely applied in healthcare [Bro+16], finance [Zha18], and politics [IK16] is to use proxy attributes in place of true attributes. Proxy methods have been immensely effective in evaluating and controlling for traditional *parity*-based notions of fairness [Dia+22; BYS24; Awa+21; Pro+21; Zha+22; AKM20; Gup+18; KMZ22], such as demographic parity [CKP09], equalized odds [HPS16], and disparate mistreatment [Zaf+17], which all aim to equalize model statistics across protected groups.

While enforcing parity is desirable in some settings, it can also lead to undesirable trade-offs. For instance, in breast cancer screening, incidence rates vary by age, with older women generally at higher risk than younger women [Kim+25]. Thus, equalizing a model’s false positive rates across age groups, for example, might reduce the sensitivity of cancer detection in older women, who are more likely to have the disease. Conversely, equalizing false negative rates might lead to unnecessary biopsies by increasing false positive rates in certain groups. Instead of equalizing model statistics across groups, a more appropriate fairness criterion would be to ask that the model’s risk predictions approximately reflect true probabilities within each age group.

These challenges have led to the development of two newer fairness notions: multiaccuracy and multicalibration [KGZ19; Gop+22; Héb+18]. Instead of enforcing parity, these methods ensure that model predictions are unbiased and well-calibrated across groups. They can be applied to complex, overlapping sensitive groups—such as those defined by race and gender—while maintaining high predictive accuracy and ensuring the model remains useful in practice, offering significant advantages over traditional parity-based metrics. As a result, enforcing multiaccuracy or multicalibration can often be preferable in many contexts [KGZ19; Héb+18]. However, a key challenge remains: how can we build provably multiaccurate and multicalibrated models leveraging proxy attributes when sensitive group data is missing?

Tackling this issue is essential for developing models that are fair across multiple complex groups without sacrificing accuracy or utility. In this work, we address this gap. We study how to estimate multiaccuracy and multicalibration fairness violations without access to true sensitive at-

tributes. We show that proxy-sensitive attributes can be used to derive computable upper bounds on these violations, capturing the model’s worst-case fairness. Additionally, we demonstrate that post-processing a model to satisfy multiaccuracy or multicalibration across proxies effectively reduces these upper bounds, offering practical utility. In conclusion, we demonstrate that even when sensitive information is incomplete or inaccessible, proxies can extend approximate multiaccuracy and multicalibration protections in a meaningful way.

1.1 Related Work

Using proxy-sensitive attributes to measure and enforce model fairness has been extensively studied for various parity-based fairness notions.

Measuring fairness. Measuring a model’s true fairness through proxies has become an important area of research. Chen et al. [Che+19] were among the first to tackle this challenge by studying the error in measuring demographic parity using proxies derived from thresholding the Bayes optimal predictor for the sensitive attribute. Awasthi et al. [Awa+21] focus on equalized odds, identifying key properties that proxies must satisfy to accurately estimate true equalized odds disparities. Kallus, Mao, and Zhou [KMZ22] further examine the ability to identify traditional parity-based fairness violations. They demonstrate that, under general assumptions about the distribution and classifiers, it is usually impossible to pinpoint fairness violations accurately using proxies. Additionally, by assuming access to the Bayes optimal predictor for the sensitive attribute, they provide tight upper and lower bounds on various fairness criteria, thereby characterizing the feasible regions for these violations. More generally, considering any proxy model instead of the Bayes optimal, Zhu et al. [Zhu+23] shows that estimating true parity-based fairness disparities using proxies results in errors proportional to the proxy error and the true fairness disparity. Most recently, Bharti, Yi, and Sulam [BYS24] address a setting with more limited information compared to [Zhu+23], providing computable and actionable upper bounds on true equalized odds disparities based on the proxy’s error and group-wise model statistics with respect to the proxies.

Enforcing fairness. An equally important question is how to ensure fairness using proxies. Awasthi, Kleindessner, and Morgenstern [AKM20] examine the post-processing method for equalized odds [HPS16] when noisy proxies are used instead of true sensitive attributes. They show that, under conditional independence assumptions, using proxies in the post-processing method results in a predictor with reduced equalized odds disparity. Wang et al. [Wan+20], working with a slightly different noise model, propose robust optimization approaches to train fair models using noisy sensitive features. Having proven that fairness violations are often unidentifiable, Kallus, Mao, and Zhou [KMZ22] take a different approach and focus on reducing the worst-case violations. Under additional smoothness assumptions they derive tighter feasible regions for fairness disparities, offering improved worst-case guarantees for fairness violations. More recently, Bharti, Yi, and Sulam [BYS24] characterize the predictor that has optimal worst-case violations and provide a generalized version of Hardt, Price, and Srebro [HPS16]’s method that returns such a predictor. Taking a different perspective, Lahoti et al. [Lah+20] avoid relying on proxies altogether. Instead, they propose solving a minimax optimization problem over a vast set of subgroups, reasoning that any good proxy for a sensitive feature would naturally be included in this set. Diana et al. [Dia+22] address the problem of learning proxies that enable downstream model developers to train models that satisfy common parity-based fairness notions. They demonstrate that this entails constructing a multiaccurate proxy and introduce a general oracle-efficient algorithm to learn such proxies.

1.2 Our Contributions

There exists a rich line of work that studies how to evaluate and enforce parity-based notions of fairness when sensitive attribute data is missing via proxies. These, however, do not extend to settings where multiaccuracy and multicalibration are more appropriate, limiting their applicability in data-scare regimes. In this work, we address this issue. Our main contributions are the following:

1. We study the problem of estimating multiaccuracy and multicalibration violations of a fixed model without access to sensitive group information.
2. We derive computable upper bounds for multiaccuracy and multicalibration violations using proxy-sensitive attributes.
3. We show that post-processing a model to satisfy multiaccuracy and multicalibration across proxies reduces these worst-case violations, allowing us to extend fairness protections without full group data.

Organization. The remainder of the paper is structured as follows. In Section 2, we introduce the necessary notation and formalize the setting. Section 3 provides background on multiaccuracy and multicalibration. Our main theoretical results are presented in Section 4 and Section 5, where we establish computable upper bounds on violations and demonstrate how to minimize them. Experimental results are detailed in Section 6. Finally, we conclude in Section 7 discussing implications of our work and closing remarks.

2 Setting and Background

Notation. We consider a binary classification setting¹ with a data distribution \mathcal{D} supported on $\mathcal{X} \times \mathcal{Z} \times \mathcal{Y}$, where $\mathcal{X} \subseteq \mathbb{R}^d$ represents the d -dimensional feature space, $\mathcal{Y} = \{0, 1\}$ denotes the binary label space, and $\mathcal{Z} \subseteq \mathbb{R}^K$ is the K -dimensional sensitive group space. For an individual represented by the pair (X, Z) , X is a vector of features and $Z = (Z_1, \dots, Z_K)$ is a vector of the individual’s sensitive attributes that allows us to determine their membership in K basic groups (e.g., age, race, biological sex). We denote $\mathcal{G} = \{g : \mathcal{X} \times \mathcal{Z} \rightarrow \{0, 1\}\}$ as the set of functions that define complex, potentially intersecting, groups in $\mathcal{X} \times \mathcal{Z}$. For any $g \in \mathcal{G}$, $g(X, Z) = 1$ indicates that the individual X belongs to group g . For example, let X_1 be an individual’s credit score and let Z_1 and Z_2 represent the individual’s age and membership in the African American racial group. Then, $g(X, Z) = \mathbf{1}\{X_1 > 700 \wedge Z_1 \geq 40 \wedge Z_2 = 1\}$ specifies the group of all African Americans, 40 years or older, with a credit score over 700. In this way, it is easy to define complex, overlapping groups defined by the intersection of basic attributes and other features. Finally, in our setting, a model is a function $f : \mathcal{X} \rightarrow [0, 1]$ that maps from the feature space to the interval $[0, 1]$. We denote its image as $\text{Im}(f) = \{f(X) : X \in \mathcal{X}\}$ and assume that $|\text{Im}(f)| < \infty$.

Problem Setting. In this work, the primary objective is to assess whether a model f is fair with respect to a set of sensitive groups \mathcal{G} *without* having access to the functions in \mathcal{G} to determine group membership. Formally, and similar to previous work [Awa+21; KMZ22], we consider a setting where we do not have access to samples (X, Z, Y) from the complete distribution \mathcal{D} . Thus, we are unable to use the true set of grouping functions \mathcal{G} as their domain is supported on $\mathcal{X} \times \mathcal{Z}$. Instead, we assume access to samples (X, Y) from the marginal distribution over $\mathcal{X} \times \mathcal{Y}$, denoted as $\mathcal{D}_{\mathcal{X}\mathcal{Y}}$ allowing us to evaluate the overall performance of f via its mean-squared error

$$\text{MSE}(f) = \mathbb{E}_{(X, Y) \sim \mathcal{D}_{\mathcal{X}\mathcal{Y}}}[(Y - f(X))^2]. \quad (1)$$

¹One can also extend this to a K -class problem using a one-vs-all approach.

Additionally, we assume a proxy developer has access to samples (X, Z) from the marginal distribution of \mathcal{D} over $\mathcal{X} \times \mathcal{Z}$, denoted as $\mathcal{D}_{\mathcal{X}\mathcal{Z}}$. The proxy developer provides us a set of learned proxy functions $\hat{\mathcal{G}} = \{\hat{g} : \mathcal{X} \rightarrow \{0, 1\}\}$ for \mathcal{G} (one for each g) that only use features X , which allows us to utilize them to determine proxy group membership. Moreover, via the proxy developer, we know how well any proxy $\hat{g} \in \hat{\mathcal{G}}$ approximates its associated true $g \in \mathcal{G}$ through its misclassification error,

$$\text{err}(\hat{g}) = \mathbb{P}_{(X,Z) \sim \mathcal{D}_{\mathcal{X}\mathcal{Z}}}[\hat{g}(X) \neq g(X, Z)]. \quad (2)$$

With this setup, we are modeling real-world situations where we lack information about individuals' basic sensitive attributes, such as sex and race. In doing so, it also prevents us from accurately identifying individuals' membership in complex intersecting groups (for example, white women over the age of 40). Instead, we rely on proxies that we can use to represent all groups and, importantly, we do not make stringent, unverifiable assumptions about these proxies, unlike other studies [Pro+21; AKM20; Awa+21]; we only consider knowing their error rates, $\text{err}(\hat{g})$.

With our setting fully described, we now turn to our main objective: assessing the fairness of the model f with respect to \mathcal{G} . Specifically, we focus on two fairness concepts—multiaccuracy and multicalibration—which we now formally define.

3 Multiaccuracy and Multicalibration

Multiaccuracy. Multiaccuracy (MA) is a notion of fairness originally introduced by [KGZ19; Héb+18]. For any sensitive group $g \in \mathcal{G}$, MA evaluates the bias of a model f , conditional on membership in g via

$$\text{AE}_{\mathcal{D}}(f, g) = \left| \mathbb{E}[g(X, Z)(f(X) - Y)] \right| \quad (3)$$

and requires that $\text{AE}_{\mathcal{D}}(f, g)$ be small for all groups.

Definition 3.1 (Multiaccuracy [KGZ19]). Fix a distribution \mathcal{D} and let \mathcal{G} be a set of groups. A model f is (\mathcal{G}, α) -multiaccurate if

$$\text{AE}_{\mathcal{D}}^{\max}(f, \mathcal{G}) := \max_{g \in \mathcal{G}} \text{AE}_{\mathcal{D}}(f, g) \leq \alpha \quad (4)$$

(\mathcal{G}, α) -multiaccuracy requires that the predictions of f be approximately unbiased overall *and* on every group. Building on this, [Héb+18] introduced a stronger notion of group fairness known as multicalibration (MC), which demands unbiased *and* calibrated predictions. Central to evaluating multicalibration is the expected calibration error (ECE) for a group $g \in \mathcal{G}$

$$\text{ECE}_{\mathcal{D}}(f, g) = \mathbb{E} \left[\left| \mathbb{E}[g(X, Z)(f(X) - Y) | f(X) = v] \right| \right].$$

where the outer expectation is over $v \sim \mathcal{D}_f$, the distribution of predictions made by the model f under \mathcal{D} . Multicalibration requires that $|\text{ECE}_{\mathcal{D}}(f, g)|$ be small for all groups.

Definition 3.2 (Multicalibration [Héb+18]). Fix a distribution \mathcal{D} and let \mathcal{G} be a set of groups. A model f is (\mathcal{G}, α) -multicalibrated if

$$\text{ECE}_{\mathcal{D}}^{\max}(f, \mathcal{G}) := \max_{g \in \mathcal{G}} \text{ECE}_{\mathcal{D}}(f, g) \leq \alpha. \quad (5)$$

(\mathcal{G}, α) -multicalibration requires that predictions of our model f be approximately unbiased and calibrated on all groups defined by \mathcal{G} .

Having presented these definitions, the problem we face is now clear: Ideally, we would evaluate $\text{AE}_{\mathcal{D}}^{\max}$ and $\text{ECE}_{\mathcal{D}}^{\max}$. However, this requires access to samples $(X, Z, Y) \sim \mathcal{D}$ and the functions \mathcal{G} , neither of which we assume to have. As alluded to before, no method exists that can guarantee—let alone, correct—that a predictor is (\mathcal{G}, α) -multiaccurate or multicalibrated in the absence of ground truth group attributes. Fortunately, in the following sections, we demonstrate that proxies can effectively circumvent these limitations and provide meaningful guarantees.

4 Bounds on Multigroup Fairness Violations

We will now demonstrate that it is still possible to derive computable and useful upper bounds for how multiaccurate and multicalibrated a model f is across the true groups \mathcal{G} , even in the absence of that information. Our first result provides computable upper bounds on $\text{AE}_{\mathcal{D}}(f, g)$ and $\text{ECE}_{\mathcal{D}}(f, g)$ for any group g .

Lemma 4.1. *Fix a distribution \mathcal{D} and model f . For any group g and its corresponding proxy \hat{g} ,*

$$\text{AE}_{\mathcal{D}}(f, g) \leq F(f, \hat{g}) + \text{AE}_{\mathcal{D}}(f, \hat{g}) \quad (6)$$

$$\text{ECE}_{\mathcal{D}}(f, g) \leq F(f, \hat{g}) + \text{ECE}_{\mathcal{D}}(f, \hat{g}) \quad (7)$$

where

$$F(f, \hat{g}) = \min \left(\text{err}(\hat{g}), \sqrt{\text{MSE}(f) \cdot \text{err}(\hat{g})} \right) \quad (8)$$

A proof of this result is provided in Appendix B.1. In our setting, both bounds can be directly evaluated. To see this, note first that we have access to $\text{err}(\hat{g})$ for all $g \in \mathcal{G}$. Second, given samples (X, Y) , we can compute $\text{MSE}(f)$ and, using proxies $\hat{\mathcal{G}}$, evaluate $\text{AE}_{\mathcal{D}}(f, \hat{g})$ and $\text{ECE}_{\mathcal{D}}(f, \hat{g})$. This result aligns with intuition, showing how the interaction between a proxy \hat{g} and model f constrains the maximum possible values of $\text{AE}_{\mathcal{D}}(f, g)$ and $\text{ECE}_{\mathcal{D}}(f, g)$. If the proxy \hat{g} is highly accurate in that it predicts g better than f predicts Y , i.e.,

$$\text{err}(\hat{g}) < \text{MSE}(f), \quad (9)$$

then $F(f, \hat{g}) = \text{err}(\hat{g})$, and the true violations $\text{AE}_{\mathcal{D}}(f, \hat{g})$ and $\text{ECE}_{\mathcal{D}}(f, \hat{g})$ are approximately bounded by their proxy estimates, achieving equality when $\text{err}(\hat{g}) = 0$. Conversely, if f is highly accurate in predicting Y but the proxy is weaker, so that

$$\text{MSE}(f) < \text{err}(\hat{g}), \quad (10)$$

then $F(f, \hat{g}) = \sqrt{\text{MSE}(f) \cdot \text{err}(\hat{g})}$, and one can attain a better bound by adding $\sqrt{\text{MSE}(f) \cdot \text{err}(\hat{g})}$. This aligns with intuition: as $\text{MSE}(f)$ decreases, the maximum values of $\text{AE}_{\mathcal{D}}(f, \hat{g})$ and $\text{ECE}_{\mathcal{D}}(f, \hat{g})$ also decrease. Consequently, the bias and expected calibration error on any group g will be small, as expected. Most importantly, with this result, we can provide an upper bound for the true MA and MC violations of f across \mathcal{G} .

Theorem 4.2. *Fix a distribution \mathcal{D} and model f . Let \mathcal{G} be a set of true groups and $\hat{\mathcal{G}}$ be its associated set of proxy groups. Then, f is $(\mathcal{G}, \beta(f, \hat{\mathcal{G}}))$ -multiaccurate and $(\mathcal{G}, \gamma(f, \hat{\mathcal{G}}))$ -multicalibrated where*

$$\beta(f, \hat{\mathcal{G}}) = \max_{\hat{g} \in \hat{\mathcal{G}}} F(f, \hat{g}) + \text{AE}_{\mathcal{D}}(f, \hat{g}) \quad (11)$$

$$\gamma(f, \hat{\mathcal{G}}) = \max_{\hat{g} \in \hat{\mathcal{G}}} F(f, \hat{g}) + \text{ECE}_{\mathcal{D}}(f, \hat{g}) \quad (12)$$

Algorithm 1 Multiaccuracy Regression

- 1: **Input:** Initial model f and set of groups \mathcal{G}
- 2: Solve

$$\begin{aligned} \hat{f} &\in \arg \min_{\lambda \in \mathbb{R}^{|\mathcal{G}|}} \text{MSE}(\hat{f}) \\ \text{s.t. } \hat{f}(X, Z) &= f(X) + \sum_{g \in \mathcal{G}} \lambda_g \cdot g(X, Z) \end{aligned}$$

- 3: Return \hat{f}
-

This result directly follows from Lemma 4.1, with a complete proof provided in Appendix B.2. It is particularly valuable because, even without directly evaluating the quantities of interest, $\text{AE}_{\mathcal{D}}^{\max}(f, \mathcal{G})$ and $\text{ECE}_{\mathcal{D}}^{\max}(f, \mathcal{G})$, we can still assess these *worst-case* violations, which offer practical utility. For instance, if we need to ensure that f is (\mathcal{G}, α) -multicalibrated before deployment, we can proceed confidently even without direct access to \mathcal{G} , provided that $\gamma(f, \hat{\mathcal{G}}) < \alpha$. Conversely, if the worst-case violations are large, this suggests that f may *potentially* be significantly biased or uncalibrated for certain groups g .

As model developers, we should pause deployment and then ask: if one instead observed that $\gamma(f, \hat{\mathcal{G}}) > \alpha$, could we reduce the bounds on multiaccuracy and multicalibration errors of f ? We show that it is possible in the following section.

5 Reducing Worst-Case Violations

The results from the previous section allow us to upper bound MA and MC violations using proxies. Now, we show that these violations can be provably reduced, yielding stronger worst-case guarantees. Recall that we have a fixed set of proxies $\hat{\mathcal{G}}$, a model f , and access to samples (X, Y) . Within the bounds $\beta(f, \hat{\mathcal{G}})$ and $\gamma(f, \hat{\mathcal{G}})$, there are only two quantities we can modify by adjusting f : the mean squared error $\text{MSE}(f)$ and either $\text{AE}_{\mathcal{D}}(f, \hat{g})$ or $\text{ECE}_{\mathcal{D}}(f, \hat{g})$. Since we lack access to (X, Z) and the true grouping functions \mathcal{G} , we cannot reduce the proxy errors $\text{err}(\hat{g})$. Thus, the question is, what modifications should be made to f such that the updated model, \hat{f} , has smaller bounds? We answer this question for the bound on multicalibration in the following theorem.

Theorem 5.1. *Fix a distribution \mathcal{D} , initial model f , and set of proxy groups $\hat{\mathcal{G}}$. If a model \hat{f} satisfies*

$$\text{ECE}_{\mathcal{D}}^{\max}(\hat{f}, \hat{\mathcal{G}}) < \min_{\hat{g} \in \hat{\mathcal{G}}} \text{ECE}_{\mathcal{D}}(f, \hat{g}) \tag{13}$$

$$\text{MSE}(\hat{f}) \leq \text{MSE}(f) \tag{14}$$

then, it will have a smaller worst-case multicalibration violation, i.e.

$$\gamma(\hat{f}, \hat{\mathcal{G}}) \leq \gamma(f, \hat{\mathcal{G}}). \tag{15}$$

An identical result for multiaccuracy is given in Appendix A, with a proof for both results provided in Appendix B.3. In simple terms, this result states that if we can obtain a new model \hat{f} that 1) is multicalibrated with respect to $\hat{\mathcal{G}}$ at level $\alpha = \min_{\hat{g} \in \hat{\mathcal{G}}} \text{ECE}_{\mathcal{D}}(f, \hat{g})$ and 2) has smaller MSE, then it is guaranteed to have a smaller worst-case violation. Fortunately, both objectives can be achieved using Algorithm 1, proposed by Gopalan et al. [Gop+22], and Algorithm 2, introduced by Roth [Rot22], which produce multiaccurate and multicalibrated predictors, respectively.

Algorithm 2 Multicalibration Boosting

- 1: **Input:** Initial model f , set of groups \mathcal{G} , and $\alpha > 0$
- 2: Let $m = \lceil \frac{1}{\alpha} \rceil, t = 0, f_0 := f$
- 3: **while**

$$\max_{g \in \mathcal{G}} \mathbb{P}[g(X, Z) = 1] \cdot \mathbb{E}[\Delta_{v,g}^2 | g(X, Z) = 1] > \alpha$$

- 4: Set

$$\begin{aligned} p_{g,v} &= \mathbb{P}[g(X, Z) = 1, f_t(X) = v] \\ (v_t, g_t) &= \arg \max_{v \in [\frac{1}{m}], g \in \mathcal{G}} p_{g,v} \cdot \Delta_{v,g}^2 \geq \alpha \\ S_{v_t, g_t} &= \{X \in \mathcal{X} : f_t(X) = v, g_t(X, Z) = 1\} \\ \tilde{v}_t &= \mathbb{E}[Y | f_t(X) = v_t, g_t(X, Z) = 1] \\ v'_t &= \arg \min_{v \in [\frac{1}{m}]} |\tilde{v}_t - v| \\ f_{t+1}(X) &= \begin{cases} v'_t, & \text{if } X \in S_{v_t, g_t} \\ f_t(X) & \text{otherwise} \end{cases} \\ t &= t + 1 \end{aligned}$$

- 5: **end while**

- 6: Let $T := t, \hat{f} := f_T$
 - 7: Return \hat{f}
-

Algorithm 1 outlines a simple algorithm for multiaccuracy. The following theorem establishes that the algorithm produces a model \hat{f} that satisfies multiaccuracy while also guaranteeing an improvement or no deterioration in MSE.

Theorem 5.2. *Fix a distribution \mathcal{D} , predictor f , and set of groups \mathcal{G} . Algorithm 1 returns a model \hat{f} that is $(0, \mathcal{G})$ -multiaccurate. Moreover,*

$$\text{MSE}(\hat{f}) \leq \text{MSE}(f). \quad (16)$$

A proof of this result can be found in [Det+24], with finite-sample guarantees discussed in [Rot22]. Algorithm 1 updates the model \hat{f} by solving a standard linear regression problem, where the features are the predictions of the initial model f and the group functions g .

While Algorithm 1 solves a convex optimization problem to generate a multiaccurate model in a single step, Algorithm 2 is an iterative method to ensure multicalibration. Algorithm 2 starts by checking if f is α -multicalibrated via the *group average squared calibration error*

$$\mathbb{E}[\Delta_{v,g}^2 | g(X, Z) = 1] \quad (17)$$

where $\Delta_{v,g} = \mathbb{E}[Y - f(X) | f(X) = v, g(X, Z) = 1]$. If this exceeds α , it identifies the conditioning event where the calibration error is the largest and refines f 's predictions. It iterates like this until convergence and this process returns a new model \hat{f} that is multicalibrated and has lower MSE than the initial model f .

Theorem 5.3. *Fix a distribution \mathcal{D} , predictor f and set of groups \mathcal{G} . Algorithm 2 stops after $T < \frac{4}{\alpha^4}$ rounds and returns model \hat{f} that is $(\sqrt{\alpha}, \mathcal{G})$ -multicalibrated. Moreover,*

$$\text{MSE}(\hat{f}) \leq \text{MSE}(f) + (1 - T) \frac{\alpha^2}{4} + \alpha \quad (18)$$

Group	$\text{err}(\hat{g})$	Group	$\text{err}(\hat{g})$	Group	$\text{err}(\hat{g})$
Black Women	0.027	Black Women	0.005	Women	0.027
White Women	0.122	White Women	0.046	White	0.092
Asian	0.06	Asian	0	Asian	0.068
Seniors	0	Multiracial	0	Black	0.039
Women	0	Black Adults	0	Asian Men	0.039
Multiracial	0.047	Women	0.079	Black Women	0.020

Table 1: Proxy errors for ACSIncome

Table 2: Proxy errors for ACSPubCov

Table 3: Proxy errors for CheXpert

A proof, along with finite-sample guarantees can be found in [Glo+23a; Rot22]. Having introduced these algorithms for obtaining multiaccurate and multicalibrated models \hat{f} , we now have a direct path to reducing worst-case violations. By applying Algorithm 1 or Algorithm 2 (at an appropriate level α) to our initial model f using the proxies $\hat{\mathcal{G}}$ —that is, enforcing multiaccuracy or multicalibration with respect to the proxies—we can systematically reduce worst-case violations on the true groups \mathcal{G} . This simple yet effective approach ensures stronger fairness guarantees and more reliable predictions across subpopulations.

6 Experimental Results

We illustrate various aspects of our theoretical results on two tabular datasets, ACSIncome and ACSPublicCoverage [Din+21], as well as on the CheXpert medical imaging dataset [Irv+19]. For the ACS datasets, we use a fixed 10% of the samples as the evaluation set. The remaining 90% of the data is split into training and validation sets, with 60% used for training the model f and proxies $\hat{\mathcal{G}}$ and 30% for adjusting f . All reported results are averages over five train/validation splits on the evaluation set. For CheXpert, we use the splits provided by [Glo+23b] for training, calibration, and evaluation. The results and metrics are computed on the evaluation set. We report results for multicalibration in the main body of the paper and defer those for multiaccuracy to Appendices C and E due to space limitations—and because multiaccuracy is a stronger notion that also implies multiaccuracy.

6.1 ACS Experiments

For the two following tabular data experiments we use the ACS dataset, a larger version of the UCI Adult dataset. In particular, we use the 2018 California data, which contains approximately 200,000 samples. We follow Hansen et al. [Han+24], and define multiple sensitive groups \mathcal{G} using basic sensitive attributes Z (e.g., **sex** and **race**, which model developers aim not to discriminate towards), along with certain features X (e.g., **age**). Examples of groups $g \in \mathcal{G}$ include **white women** and **black adults**. For both experiments, we simulate missing sensitive attributes by excluding some Z_i from the data we use to train our model f . Instead, with an auxiliary dataset of samples (X, Z) and the true set of grouping functions \mathcal{G} , we obtain a set of proxy functions $\hat{\mathcal{G}}$ to approximate \mathcal{G} .

For our initial model f , we report the worst-case violations, which we *can* evaluate in our setting. To demonstrate that enforcing multiaccuracy and multicalibration with respect to $\hat{\mathcal{G}}$ provably reduces our upper bounds, we apply Algorithm 1 and Algorithm 2 to obtain an adjusted predictor f_{adj} and report its worst-case violations as well. Additionally, for both the initial model f and

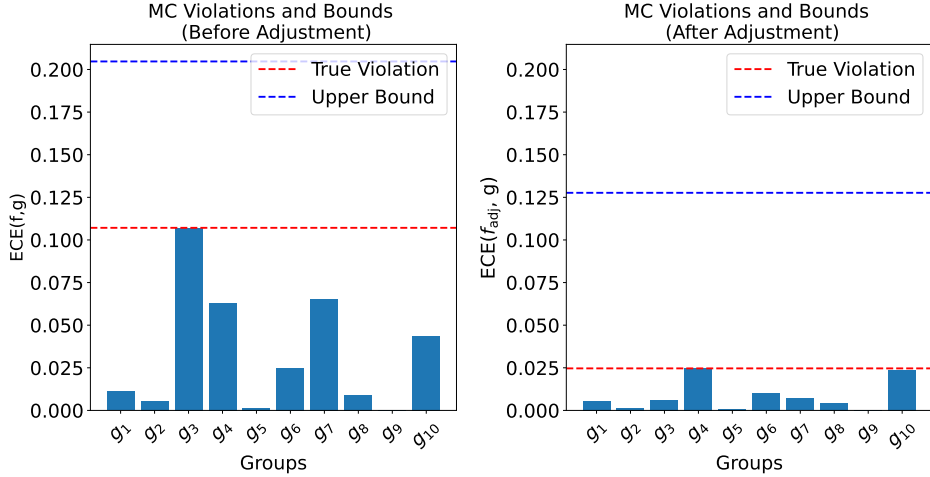


Figure 1: ECE, ECE^{\max} (dotted red line), and worst case violations (dotted blue line) of the original model f and adjusted model f_{adj} on ACS Income. Here, f is a decision tree.

adjusted model f_{adj} we report the AE and ECE, *with respect to the true groups* $g \in \mathcal{G}$, along with their maximums, AE^{\max} and ECE^{\max} . Recall that in our setting, we *cannot* actually evaluate these quantities but we report them to showcase that they lie under our bounds, illustrating the validity of our theoretical results. For these tabular experiments, we model f with a logistic regression model, a decision tree, and Random Forest. We report the results for the decision tree and defer the results of other models to Appendices C and E.

6.1.1 ACSIncome

For this experiment, we consider the task of predicting whether US working adults living in California have a yearly income exceeds \$50,000. Examples of features X include **occupation** and **education**, and here we exclude the **race** attribute.

In Table 1, we report the errors of the learned proxies $\hat{\mathcal{G}}$ for specific groups. For groups that do not depend on **race**, such as **seniors** and **women**, their respective proxies \hat{g} are perfectly accurate, exhibiting zero misclassification error. However, for groups like **multiracial** and **white women**, the proxies exhibit some error, albeit small. This proves to be useful in providing meaningful guarantees on how multiaccurate and multicalibrated our model f will be with respect to the true (but unobserved) groups \mathcal{G} .

Fig. 1 showcases the utility of our bounds. Notably, the worst-case violation (dotted red line) allows us to certify that the initial model is approximately 0.21-multicalibrated with respect to the true groups \mathcal{G} . This is indeed practically useful, as it enables practitioners to obtain fairness guarantees without having true group information. Additionally, the right-hand graph in Fig. 1 highlights the benefit of applying Algorithm 2 to multicalibrate the initial model f with respect to the proxy groups $\hat{\mathcal{G}}$. After adjusting f , the upper bound decreases, allowing us to certify that the resulting model f_{adj} is approximately 0.13-multicalibrated—a substantial improvement of 38%.

6.1.2 ACSPublicCoverage (ACSPubCov)

In this experiment, we consider the task of predicting whether low-income individuals, not eligible for Medicare, have coverage from public health insurance. Examples of features X include **age**, **education**, **income**, and more. For this experiment, we exclude the **sex** attribute.

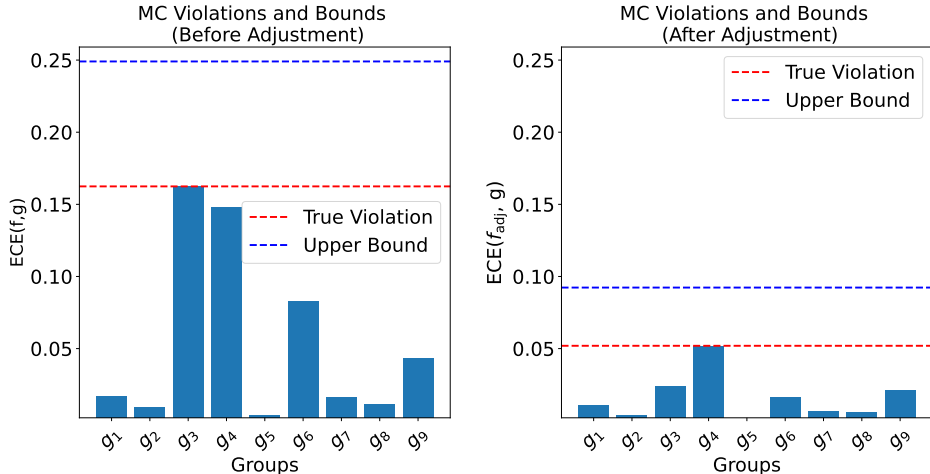


Figure 2: ECE, ECE^{\max} (dotted red line), and worst case violations (dotted blue line) of the original model f and updated model f_{adj} on ACSPubcov. Here, f is a decision tree.

In Table 2, we report the errors of the learned proxies $\hat{\mathcal{G}}$ for specific groups. Notably, for groups independent of **sex**, such as **asian** and **multiracial**, the proxies \hat{g} are perfectly accurate, exhibiting zero misclassification error. However, for groups like **black women** and **white women**, the proxies exhibit some error, though they are small. This arises because, although the proxies functions \hat{g} are not explicit functions of **sex** attribute, there exists a feature, **fertility**, that indicates whether an individual has given birth within the past 12 months and serves as a good predictor of **sex**. This demonstrates that even when sensitive attributes are missing, in many real-world setting strong proxies can still enable us to determine true sensitive group membership with high accuracy.

In Fig. 2, we show the results of applying Algorithm 2 to multicalibrate the initial model f with respect to the proxy groups $\hat{\mathcal{G}}$. Notably, our approach allows for the certification that the initial model is approximately 0.25-multicalibrated with respect to the true groups \mathcal{G} despite not having access to them. This result highlights the utility of our method, as it enables practitioners to obtain performance guarantees without needing the true group information. Furthermore, after applying multicalibration to f , the resulting model f_{adj} is certified to be approximately 0.09-multicalibrated, thereby providing a stronger guarantee.

6.2 CheXpert

CheXpert is a large public dataset of chest radiographs, with labeled annotations for 14 observations (positive, negative, or unlabeled) including **cardiomegaly**, **atelectasis**, **consolidation**, and several others. The dataset contains self-reported sensitive attributes including **race**, **sex**, and **age**. Following the set up of [Glo+23b], we work with a sample containing a total of 127,118 chest X-ray scans and consider the task of predicting the presence of **pleural effusion** in the X-rays.

We consider all 14 groups that can be made from conjunctions of **sex** and **race**. Examples of groups $g \in \mathcal{G}$ include **black men**, **asian women**, **white women**, etc. In this example, we assume that we do not have direct knowledge of patient’s self-reported **sex** or **race** when training or evaluating our model f (as it is common for privacy reasons). Instead, with an auxiliary dataset with samples (X, Z) we use the X-ray features to learn proxy models for **sex** and **race**. We then use them to construct proxies for all conjunctions as well. In Table 3, we report the proxy errors for specific groups.

We consider three different models for f . The first is a decision tree classifier trained on features

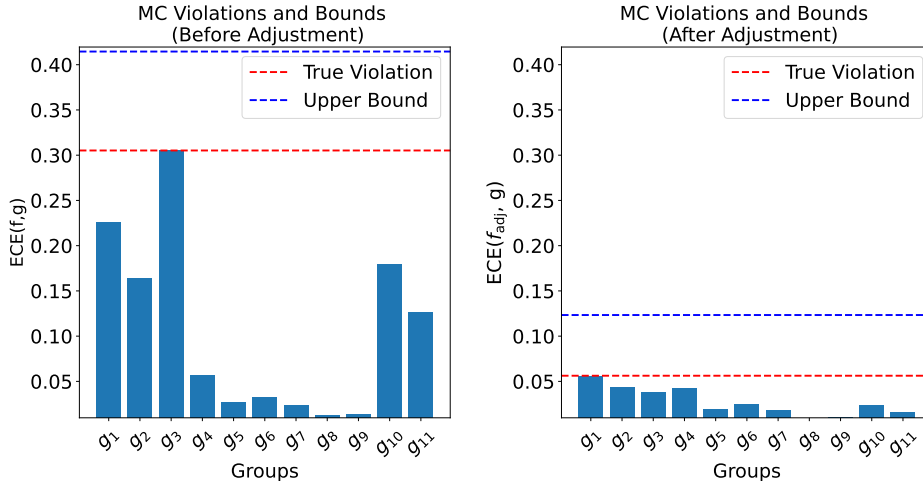


Figure 3: ECE, ECE^{\max} (dotted red line), and worst case violations (dotted blue line) of the original model f and adjusted model f_{adj} on CheXpert. Here f is a decision tree trained on embeddings of a pretrained DenseNet-121.

extracted from a DenseNet-121 model [Hua+17] pretrained on ImageNet [Den+09]. The second is a linear model [Bre01] trained on the same features. The third is a DenseNet-121 model trained end-to-end on the X-ray images.

Fig. 3 illustrates the results for the decision tree model. Before any adjustments, our worst-case violation serves as an early warning that the model f may be significantly uncalibrated on certain groups, with a violation as large as $\alpha \approx 0.42$. In a medical setting like this, such a finding is crucial, as it indicates that our predictions could be either overly confident or underconfident on sensitive groups. On the other hand, the right-hand graph of Fig. 3 demonstrates the practical benefit of applying Algorithm 2 to multicalibrate the initial model f with respect to our highly accurate proxies $\hat{\mathcal{G}}$. After a straightforward adjustment, the upper bound on the worst-case violation decreases significantly, certifying that the adjusted model f_{adj} is approximately 0.13-multicalibrated with respect to the true groups.

Fig. 4 presents the results for the logistic regression and fully-trained DenseNet models. In these cases, the worst-case violations for both models indicate that they are guaranteed to be approximately 0.11 and 0.12-multicalibrated with respect to the true groups. Notably, both models are approximately 0.03-multicalibrated with respect to the proxies. As a result, further adjustments provide negligible improvements.

7 Conclusion

In this work, we address the challenge of measuring multiaccuracy and multicalibration with respect to sensitive groups when sensitive group data is missing or unobserved. By leveraging proxy-sensitive attributes, we derive actionable upper bounds on true multiaccuracy and multicalibration, offering a principled approach to assessing worst-case fairness violations. Furthermore, we demonstrate that adjusting models to be multiaccurate or multicalibrated with respect to proxy-sensitive attributes can significantly reduce these upper bounds, strengthening guarantees on multiaccuracy and multicalibration violations for the true, but unknown, sensitive groups.

Through empirical validation on real-world datasets, we show that multiaccuracy and multicalibration can be approximated even in the absence of complete sensitive group data. These findings highlight the practicality of using proxies to assess and enforce fairness in high-stakes decision-

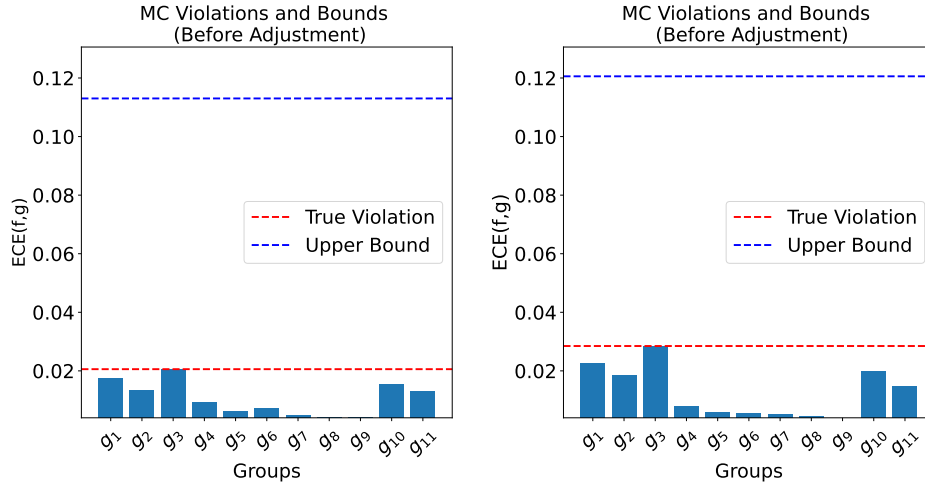


Figure 4: ECE, ECE^{\max} (dotted red line), and worst case violations (dotted blue line) of the original, unadjusted, logistic regression model (left) and trained DenseNet-121 model (right).

making contexts, where access to demographic information is often restricted. In particular, we illustrate the practical benefit of enforcing multicalibration with respect to proxies, providing practitioners with a simple and effective tool to improve fairness in their models.

Naturally, multiaccuracy and multicalibration may not be the most appropriate fairness metrics across all settings. Nonetheless, whenever these notions are relevant, our methods offer, for the first time, the possibility to certify and correct them without requiring access to ground truth group data. Lastly, note that without our recommendations of correcting for worst-case fairness with proxies, models trained on this data can inadvertently learn these sensitive attributes indirectly and base decisions on them, leading to potential negative outcomes. Our results and methodology prevent this by providing a principled approach to adjust models and reduce worst-case multiaccuracy and multicalibration violations.

Impact Statement

In this work, we propose an effective solution to a technical problem: estimating and controlling for multiaccuracy and multicalibration using proxies. While proxies can be controversial and pose risks—such as reinforcing discrimination or compromising privacy—predictive models often learn sensitive attributes indirectly, leading to unintended harm. When used carefully, proxies can help mitigate these risks, as we demonstrate in this work. However, deploying proxies in real-world scenarios requires a careful evaluation of trade-offs through discussions with policymakers, domain experts, and other stakeholders. Ultimately, proxies should be employed responsibly and solely for assessing and promoting fairness.

References

- [AKM20] Pranjal Awasthi, Matthäus Kleindessner, and Jamie Morgenstern. “Equalized odds postprocessing under imperfect group information”. In: *International Conference on Artificial Intelligence and Statistics*. PMLR. 2020, pp. 1770–1780.
- [Ang+22] Julia Angwin et al. “Machine bias”. In: *Ethics of data and analytics*. Auerbach Publications, 2022, pp. 254–264.

- [Awa+21] Pranjali Awasthi et al. “Evaluating fairness of machine learning models under uncertain and incomplete information”. In: *Proceedings of the 2021 ACM Conference on Fairness, Accountability, and Transparency*. 2021, pp. 206–214.
- [Bre01] Leo Breiman. “Random forests”. In: *Machine learning* 45.1 (2001), pp. 5–32.
- [Bro+16] David P Brown et al. “Using Bayesian imputation to assess racial and ethnic disparities in pediatric performance measures”. In: *Health services research* 51.3 (2016), pp. 1095–1108.
- [BYS24] Beepul Bharti, Paul Yi, and Jeremias Sulam. “Estimating and controlling for equalized odds via sensitive attribute predictors”. In: *Advances in neural information processing systems* 36 (2024).
- [Che+19] Jiahao Chen et al. “Fairness under unawareness: Assessing disparity when protected class is unobserved”. In: *Proceedings of the conference on fairness, accountability, and transparency*. 2019, pp. 339–348.
- [CKP09] Toon Calders, Faisal Kamiran, and Mykola Pechenizkiy. “Building classifiers with independency constraints”. In: *2009 IEEE international conference on data mining workshops*. IEEE. 2009, pp. 13–18.
- [Com21] European Commission. *Proposal for a Regulation Laying Down Harmonised Rules on Artificial Intelligence (Artificial Intelligence Act)*. 2021. URL: <https://digital-strategy.ec.europa.eu/en/policies/regulatory-framework-ai>.
- [Das22] Jeffrey Dastin. “Amazon scraps secret AI recruiting tool that showed bias against women”. In: *Ethics of data and analytics*. Auerbach Publications, 2022, pp. 296–299.
- [Den+09] Jia Deng et al. “ImageNet: A large-scale hierarchical image database”. In: *2009 IEEE conference on computer vision and pattern recognition (CVPR)*. IEEE. 2009, pp. 248–255.
- [Det+24] Gianluca Detommaso et al. “Multicalibration for confidence scoring in LLMs”. In: *Proceedings of the 41st International Conference on Machine Learning*. ICML’24. Vienna, Austria, 2024.
- [Dia+22] Emily Diana et al. “Multiaccurate Proxies for Downstream Fairness”. In: *2022 ACM Conference on Fairness, Accountability, and Transparency* (2022).
- [Din+21] Frances Ding et al. “Retiring adult: New datasets for fair machine learning”. In: *Advances in neural information processing systems* 34 (2021), pp. 6478–6490.
- [FC21] Mauricio Noris Freire and Leandro Nunes de Castro. “e-Recruitment recommender systems: a systematic review”. In: *Knowledge and Information Systems* 63 (2021), pp. 1–20.
- [Fre+16] Allen Fremont et al. “When race/ethnicity data are lacking: using advanced indirect estimation methods to measure disparities”. In: *Rand health quarterly* 6.1 (2016).
- [Glo+23a] Ira Globus-Harris et al. “Multicalibrated regression for downstream fairness”. In: *Proceedings of the 2023 AAAI/ACM Conference on AI, Ethics, and Society*. 2023, pp. 259–286.
- [Glo+23b] Ben Glocker et al. “Algorithmic encoding of protected characteristics in chest X-ray disease detection models”. In: *EBioMedicine* 89 (2023).
- [Gop+22] Parikshit Gopalan et al. “Omnipredictors”. In: *13th Innovations in Theoretical Computer Science Conference (ITCS 2022)*. Ed. by Mark Braverman. Vol. 215. Leibniz International Proceedings in Informatics (LIPIcs). Schloss Dagstuhl – Leibniz-Zentrum für Informatik, 2022.

- [GPS+23] SP Garin, VS Parekh, J Sulam, et al. “Medical imaging data science competitions should report dataset demographics and evaluate for bias [published online ahead of print April 3, 2023]”. In: *Nat Med* (2023).
- [Gup+18] Maya Gupta et al. “Proxy fairness”. In: *arXiv preprint arXiv:1806.11212* (2018).
- [Han+24] Dutch Hansen et al. “When is Multicalibration Post-Processing Necessary?” In: *Advances in Neural Information Processing Systems*. 2024.
- [Héb+18] Ursula Hébert-Johnson et al. “Multicalibration: Calibration for the (computationally-identifiable) masses”. In: *International Conference on Machine Learning*. PMLR. 2018, pp. 1939–1948.
- [Hol+19] Kenneth Holstein et al. “Improving fairness in machine learning systems: What do industry practitioners need?” In: *Proceedings of the 2019 CHI conference on human factors in computing systems*. 2019, pp. 1–16.
- [HPS16] Moritz Hardt, Eric Price, and Nati Srebro. “Equality of opportunity in supervised learning”. In: *Advances in neural information processing systems* 29 (2016).
- [Hua+17] Gao Huang et al. “Densely connected convolutional networks”. In: *Proceedings of the IEEE conference on computer vision and pattern recognition*. 2017, pp. 4700–4708.
- [IK16] Kosuke Imai and Kabir Khanna. “Improving ecological inference by predicting individual ethnicity from voter registration records”. In: *Political Analysis* 24.2 (2016), pp. 263–272.
- [Irv+19] Jeremy Irvin et al. “Chexpert: A large chest radiograph dataset with uncertainty labels and expert comparison”. In: *Proceedings of the AAAI conference on artificial intelligence*. Vol. 33. 01. 2019, pp. 590–597.
- [KGZ19] Michael P Kim, Amirata Ghorbani, and James Zou. “Multiaccuracy: Black-box post-processing for fairness in classification”. In: *Proceedings of the 2019 AAAI/ACM Conference on AI, Ethics, and Society*. 2019, pp. 247–254.
- [Kim+25] Joanne Kim et al. “Global patterns and trends in breast cancer incidence and mortality across 185 countries”. In: *Nature Medicine* (2025), pp. 1–9.
- [KMZ22] Nathan Kallus, Xiaojie Mao, and Angela Zhou. “Assessing algorithmic fairness with unobserved protected class using data combination”. In: *Management Science* 68.3 (2022), pp. 1959–1981.
- [Lah+20] Preethi Lahoti et al. “Fairness without demographics through adversarially reweighted learning”. In: *Advances in neural information processing systems* 33 (2020), pp. 728–740.
- [OM19] Ziad Obermeyer and Sendhil Mullainathan. “Dissecting racial bias in an algorithm that guides health decisions for 70 million people”. In: *Proceedings of the conference on fairness, accountability, and transparency*. 2019, pp. 89–89.
- [Pro+21] Flavien Prost et al. “Measuring model fairness under noisy covariates: A theoretical perspective”. In: *Proceedings of the 2021 AAAI/ACM Conference on AI, Ethics, and Society*. 2021, pp. 873–883.
- [Rot22] A. Roth. *Uncertain: Modern Topics in Uncertainty Estimation*. 2022.
- [RWC20] Cynthia Rudin, Caroline Wang, and Beau Coker. “The age of secrecy and unfairness in recidivism prediction”. In: *Harvard Data Science Review* 2.1 (2020), p. 1.
- [SP22] White House Office of Science and Technology Policy. *The Blueprint for an AI Bill of Rights*. 2022. URL: <https://www.whitehouse.gov/ostp/ai-bill-of-rights/>.

- [SSJ18] K Shailaja, Banoth Seetharamulu, and MA Jabbar. “Machine learning in healthcare: A review”. In: *2018 Second international conference on electronics, communication and aerospace technology (ICECA)*. IEEE. 2018, pp. 910–914.
- [TCE17] Lyn Thomas, Jonathan Crook, and David Edelman. *Credit scoring and its applications*. SIAM, 2017.
- [UU21] Scientific United Nations Educational and Cultural Organization (UNESCO). *Recommendation on the Ethics of Artificial Intelligence*. 2021.
- [Wan+20] Serena Wang et al. “Robust optimization for fairness with noisy protected groups”. In: *Advances in neural information processing systems* 33 (2020), pp. 5190–5203.
- [WH11] Joel S Weissman and Romana Hasnain-Wynia. “Advancing health care equity through improved data collection”. In: *New England Journal of Medicine* 364.24 (2011), pp. 2276–2277.
- [Zaf+17] Muhammad Bilal Zafar et al. “Fairness beyond disparate treatment & disparate impact: Learning classification without disparate mistreatment”. In: *Proceedings of the 26th international conference on world wide web*. 2017, pp. 1171–1180.
- [Zha+22] Tianxiang Zhao et al. “Towards Fair Classifiers Without Sensitive Attributes: Exploring Biases in Related Features”. In: (2022).
- [Zha18] Yan Zhang. “Assessing fair lending risks using race/ethnicity proxies”. In: *Management Science* 64.1 (2018), pp. 178–197.
- [Zhu+23] Zhaowei Zhu et al. “Weak proxies are sufficient and preferable for fairness with missing sensitive attributes”. In: *International Conference on Machine Learning*. PMLR. 2023, pp. 43258–43288.

A Additional Theoretical Results

Here we present a version of Theorem 5.1 for multiaccuracy.

Theorem A.1. *Fix a distribution \mathcal{D} , initial model f , and set of proxy groups $\hat{\mathcal{G}}$. If a model \hat{f} satisfies*

$$\text{AE}^{\max}(\hat{f}, \hat{\mathcal{G}}) < \min_{\hat{g} \in \hat{\mathcal{G}}} \text{AE}_{\mathcal{D}}(f, \hat{g}) \quad (19)$$

$$\text{MSE}(\hat{f}) \leq \text{MSE}(f) \quad (20)$$

then, it will have a smaller worst-case multiaccuracy violation, i.e. $\beta(\hat{f}, \hat{\mathcal{G}}) \leq \beta(f, \hat{\mathcal{G}})$.

A proof of this result is provided in Appendix B.3

B Proofs

B.1 Proof of Lemma 4.1

Proof. Fix a distribution \mathcal{D} and predictor f . Consider any group $g \in \mathcal{G}$ and its corresponding proxy $\hat{g} \in \hat{\mathcal{G}}$. Then,

$$\text{AE}_{\mathcal{D}}(f, g) = \left| \mathbb{E}[g(X, Z)(f(X) - Y)] \right| \quad (21)$$

$$= \left| \mathbb{E}[g(X, Z)(f(X) - Y)] - \mathbb{E}[\hat{g}(X)(f(X) - Y)] + \mathbb{E}[\hat{g}(X)(f(X) - Y)] \right| \quad (22)$$

$$\leq \left| \mathbb{E}[g(X, Z)(f(X) - Y)] - \mathbb{E}[\hat{g}(X)(f(X) - Y)] \right| + \left| \mathbb{E}[\hat{g}(X)(f(X) - Y)] \right| \quad (23)$$

$$= \left| \mathbb{E}[g(X, Z)(f(X) - Y) - \hat{g}(X)(f(X) - Y)] \right| + \text{AE}_{\mathcal{D}}(f, \hat{g}) \quad (24)$$

$$= \left| \mathbb{E}[(g(X, Z) - \hat{g}(X)) \cdot (f(X) - Y)] \right| + \text{AE}_{\mathcal{D}}(f, \hat{g}) \quad (25)$$

$$\leq \mathbb{E}[|g(X, Z) - \hat{g}(X)| \cdot |f(X) - Y|] + \text{AE}_{\mathcal{D}}(f, \hat{g}) \quad (26)$$

$$\leq \min \left(\sqrt{\mathbb{E}[|g(X, Z) - \hat{g}(X)|^2] \mathbb{E}[|f(X) - Y|^2]}, \mathbb{E}[|g(X, Z) - \hat{g}(X)|] \right) + \text{AE}_{\mathcal{D}}(f, \hat{g}) \quad (27)$$

$$= \min \left(\sqrt{\text{MSE}(f) \cdot \text{err}(\hat{g})}, \text{err}(\hat{g}) \right) + \text{AE}_{\mathcal{D}}(f, \hat{g}) \quad (28)$$

Here we applied the triangle inequality from line 20-21 and Holder's inequality from line 23-24.

Similarly

$$\text{ECE}_{\mathcal{D}}(f, g) = \mathbb{E} \left[\left| \mathbb{E}[g(X, Z)(f(X) - Y) | f(X) = v] \right| \right] \quad (29)$$

$$= \mathbb{E} \left[\left| \mathbb{E}[g(X, Z)(f(X) - Y) | f(X) = v] \right| - \left| \mathbb{E}[\hat{g}(X)(f(X) - Y) | f(X) = v] \right| \right] \quad (30)$$

$$+ \left| \mathbb{E}[\hat{g}(X)(f(X) - Y) | f(X) = v] \right| \quad (31)$$

$$= \mathbb{E} \left[\left| \mathbb{E}[g(X, Z)(f(X) - Y) | f(X) = v] \right| - \left| \mathbb{E}[\hat{g}(X)(f(X) - Y) | f(X) = v] \right| \right] + \text{ECE}_{\mathcal{D}}(f, \hat{g}) \quad (32)$$

$$\leq \mathbb{E} \left[\left| \mathbb{E}[g(X, Z)(f(X) - Y) | f(X) = v] - \mathbb{E}[\hat{g}(X)(f(X) - Y) | f(X) = v] \right| \right] + \text{ECE}_{\mathcal{D}}(f, \hat{g}) \quad (33)$$

$$= \mathbb{E} \left[\left| \mathbb{E}[g(X, Z)(f(X) - Y) - \hat{g}(X)(f(X) - Y) | f(X) = v] \right| \right] + \text{ECE}_{\mathcal{D}}(f, \hat{g}) \quad (34)$$

$$\leq \mathbb{E} \left[\left| \mathbb{E} \left[\left| g(X, Z)(f(X) - Y) - \hat{g}(X)(f(X) - Y) \right| \middle| f(X) = v \right] \right| \right] + \text{ECE}_{\mathcal{D}}(f, \hat{g}) \quad (35)$$

$$= \mathbb{E} \left[\left| g(X, Z)(f(X) - Y) - \hat{g}(X)(f(X) - Y) \right| \right] + \text{ECE}_{\mathcal{D}}(f, \hat{g}) \quad (36)$$

$$= \mathbb{E} \left[\left| (g(X, Z) - \hat{g}(X)) \cdot (f(X) - Y) \right| \right] + \text{ECE}_{\mathcal{D}}(f, \hat{g}) \quad (37)$$

$$\leq \min \left(\sqrt{\mathbb{E}[|g(X, Z) - \hat{g}(X)|^2] \cdot \mathbb{E}[|f(X) - Y|^2]}, \mathbb{E}[|g(X, Z) - \hat{g}(X)|] \right) + \text{ECE}_{\mathcal{D}}(f, \hat{g}) \quad (38)$$

$$= \min \left(\sqrt{\text{MSE}(f) \cdot \text{err}(g, \hat{g})}, \text{err}(\hat{g}) \right) + \text{ECE}_{\mathcal{D}}(f, \hat{g}) \quad (39)$$

Here we applied the triangle inequality from line 30-31 and Holder's inequality from line 35-36. \square

B.2 Proof of Theorem 4.2

Proof. We prove the result for multiaccuracy. Recall Lemma 4.1, which states that for any group g and its proxy \hat{g}

$$\text{AE}_{\mathcal{D}}(f, g) \leq F(f, \hat{g}) + \text{AE}_{\mathcal{D}}(f, \hat{g}) \quad (40)$$

Thus, $\forall g \in \mathcal{G}$,

$$\text{AE}_{\mathcal{D}}(f, g) \leq \beta(f, \hat{\mathcal{G}}) := \max_{\hat{g} \in \hat{\mathcal{G}}} F(f, \hat{g}) + \text{AE}_{\mathcal{D}}(f, \hat{g}) \quad (41)$$

which proves that f is $(\mathcal{G}, \beta(f, \hat{\mathcal{G}}))$ -multiaccurate. The proof for multicalibration follows an identical argument. \square

B.3 Proof of Theorem 5.1

Proof. Fix a distribution \mathcal{D} , model f , set of groups \mathcal{G} and its corresponding proxies $\hat{\mathcal{G}}$. Recall by Theorem 4.2 that f is $(\mathcal{G}, \gamma(f, \cdot))$ -multicalibrated where

$$\gamma(f, \hat{\mathcal{G}}) = \max_{\hat{g} \in \hat{\mathcal{G}}} \min \left(\text{err}(\hat{g}), \sqrt{\text{MSE}(f) \cdot \text{err}(\hat{g})} \right) + \text{ECE}_{\mathcal{D}}(f, \hat{g}) \quad (42)$$

First, note that for $\text{MSE}(f) > \text{err}(\hat{g})$, the term

$$\min\left(\text{err}(\hat{g}), \sqrt{\text{MSE}(f) \cdot \text{err}(\hat{g})}\right) \quad (43)$$

is constant with respect to $\text{MSE}(f)$ and for $\text{MSE}(f) \leq \text{err}(\hat{g})$ it increases as $\text{MSE}(f)$ increases.

Now, suppose another model \hat{f} satisfies the following

$$\text{ECE}^{\max}(\hat{f}, \hat{\mathcal{G}}) < \min_{\hat{g} \in \hat{\mathcal{G}}} \text{ECE}_{\mathcal{D}}(f, \hat{g}) \quad (44)$$

$$\text{MSE}(\hat{f}) \leq \text{MSE}(f). \quad (45)$$

Then,

$$\gamma(\hat{f}, \hat{\mathcal{G}}) = \max_{\hat{g} \in \hat{\mathcal{G}}} \min\left(\text{err}(\hat{g}), \sqrt{\text{MSE}(\hat{f}) \cdot \text{err}(\hat{g})}\right) + \text{ECE}_{\mathcal{D}}(\hat{f}, \hat{g}) \quad (46)$$

$$\leq \max_{\hat{g} \in \hat{\mathcal{G}}} \min\left(\text{err}(\hat{g}), \sqrt{\text{MSE}(f) \cdot \text{err}(\hat{g})}\right) + \text{ECE}_{\mathcal{D}}(\hat{f}, \hat{g}) \quad (47)$$

$$\leq \max_{\hat{g} \in \hat{\mathcal{G}}} \min\left(\text{err}(\hat{g}), \sqrt{\text{MSE}(f) \cdot \text{err}(\hat{g})}\right) + \text{ECE}^{\max}(\hat{f}, \hat{\mathcal{G}}) \quad (48)$$

$$\leq \max_{\hat{g} \in \hat{\mathcal{G}}} \min\left(\text{err}(\hat{g}), \sqrt{\text{MSE}(f) \cdot \text{err}(\hat{g})}\right) + \min_{\hat{g} \in \hat{\mathcal{G}}} \text{ECE}_{\mathcal{D}}(f, \hat{g}) \quad (49)$$

$$\leq \max_{\hat{g} \in \hat{\mathcal{G}}} \min\left(\text{err}(\hat{g}), \sqrt{\text{MSE}(f) \cdot \text{err}(\hat{g})}\right) + \text{ECE}_{\mathcal{D}}(f, \hat{g}) \quad (50)$$

$$= \gamma(f, \hat{\mathcal{G}}). \quad (51)$$

The proof of the multiaccuracy result in Theorem A.1 follows an identical argument. \square

C Additional Experiment Details

C.1 ACS Experiments

Models. In the ACSIncome and PubCov experiments, we train Random Forests for the proxies. For the models f , we train three types: logistic regression, decision tree, and Random Forest.

Results. The groups used along with proxy errors are reported in Tables 4 and 5. All multiaccuracy related results for the different models f are presented in Appendix E. Note, all of the models are multiaccurate with respect to \mathcal{G} and $\hat{\mathcal{G}}$. As a result, adjusting provides no benefit. All multicalibration related results for the different models f are presented in Appendix E. Note, the logistic regression and Random Forest models are highly multicalibrated with respect to \mathcal{G} and $\hat{\mathcal{G}}$. As a result, adjusting provides no benefit. On the other hand, the decision tree is grossly uncalibrated with respect to some proxies. As a result, we see a benefit in multicalibrating with respect to the proxies.

C.2 CheXpert

Models. In the CheXpert experiment, we follow Glocker et al. [Glo+23b] and train a DenseNet-121 model for the to predict **race** and **sex**. For the models f , we use three types. The first is a decision tree classifier trained on features extracted from a DenseNet-121 model [Hua+17] pretrained on ImageNet [Den+09]. The second is a linear model [Bre01] trained on the same features. The third is a DenseNet-121 model trained end-to-end on the raw X-ray images.

Results The groups used along with proxy errors are reported in Table 6. All multiaccuracy related results for the different types of models f are presented in Appendix E. Note, all of the models are multiaccurate with respect to \mathcal{G} and $\hat{\mathcal{G}}$. As a result, adjusting provides no benefit. All multicalibration related results for the different types of models f are presented in Appendix E. Note, the logistic regression and fully trained DenseNet-121 models are highly multicalibrated with respect to \mathcal{G} and $\hat{\mathcal{G}}$. As a result, adjusting provides no benefit. On the other hand, the decision tree is grossly uncalibrated with respect to some proxies. As a result, we see a benefit in multicalibrating with respect to the proxies.

D Additional Tables

Group	$\text{err}(\hat{g})$
Black Adults	0.044
Black Women	0.0269
Women	0
Never Married	0
American Indian	0.007
Seniors	0
White Women	0.123
Multiracial	0.047
White Children	0.002
Asian	0.060

Table 4: Groups and proxy errors for ACS Income

Group	$\text{err}(\hat{g})$
Black Adults	0.044
Black Women	0.0269
Women	0
Never Married	0
American Indian	0.007
White Women	0.123
Multiracial	0.047
White Children	0.002
Asian	0.060

Table 5: Groups and proxy errors for ACSPubCov

Group	$\text{err}(\hat{g})$
Men	0.027
Women	0.027
White	0.92
Asian	0.068
Black	0.039
Asian Men	0.039
Asian Women	0.034
Black Men	0.021
Black Women	0.020
White Men	0.067
White Women	0.062

Table 6: Groups and proxy errors for CheXpert

E Additional Figures

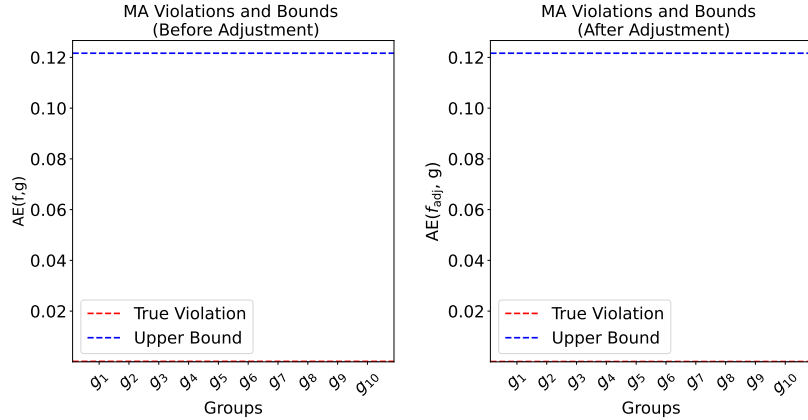


Figure B.1: $AE(f, g)$, $AE^{\max}(f, g)$ (dotted red line), and worst case violations (dotted blue line) of the original model f and adjusted model f_{adj} on ACSIncome. Here, f is a logistic regression.

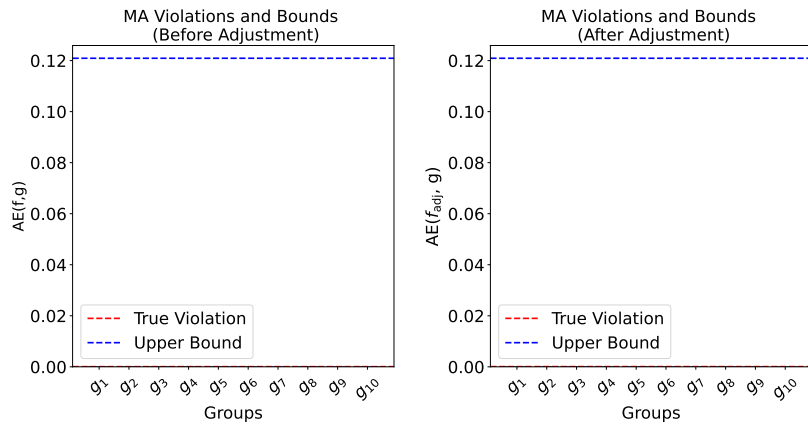


Figure B.2: $AE(f, g)$, $AE^{\max}(f, g)$ (dotted red line), and worst case violations (dotted blue line) of the original model f and adjusted model f_{adj} on ACSIncome. Here, f is a decision tree.

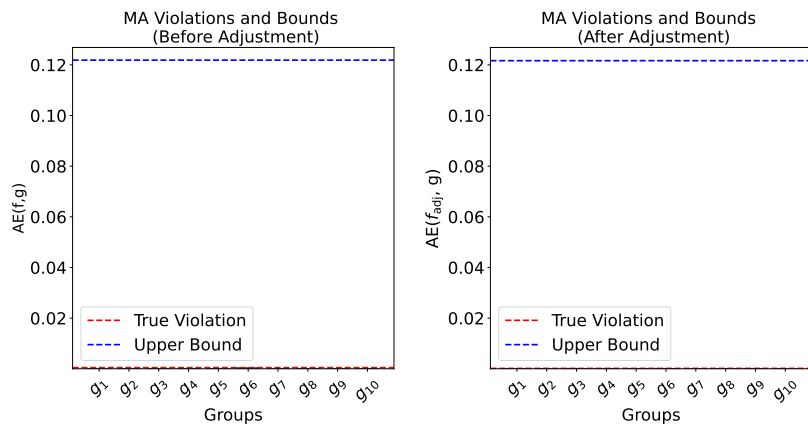


Figure B.3: $AE(f, g)$, $AE^{\max}(f, g)$ (dotted red line), and worst case violations (dotted blue line) of the original model f and adjusted model f_{adj} on ACSIncome. Here, f is a Random Forest.

Figure B.4: Multiaccuracy results for ACSIncome

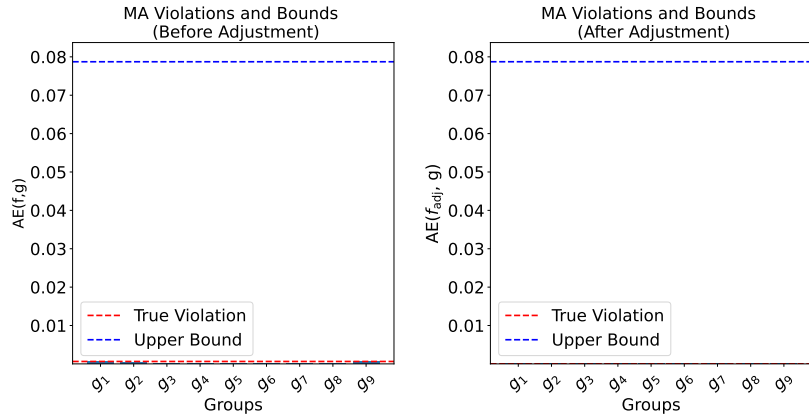


Figure B.5: $AE(f, g)$, $AE^{\max}(f, g)$ (dotted red line), and worst case violations (dotted blue line) of the original model f and adjusted model f_{adj} on ACSPubCov. Here, f is a logistic regression.

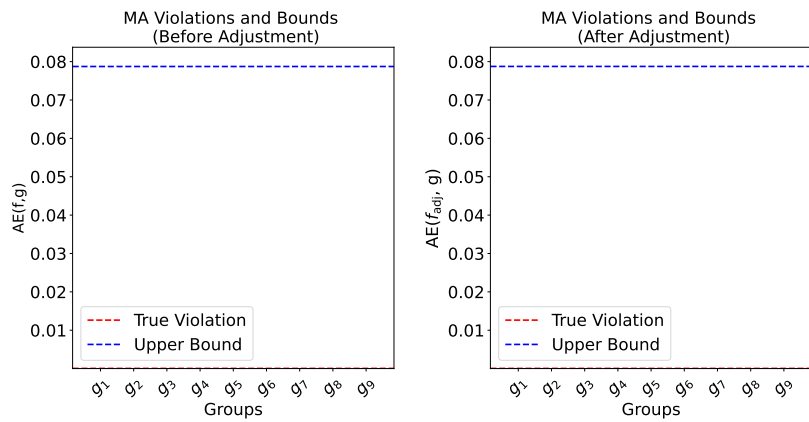


Figure B.6: $AE(f, g)$, $AE^{\max}(f, g)$ (dotted red line), and worst case violations (dotted blue line) of the original model f and adjusted model f_{adj} on ACSPubCov. Here, f is a decision tree.

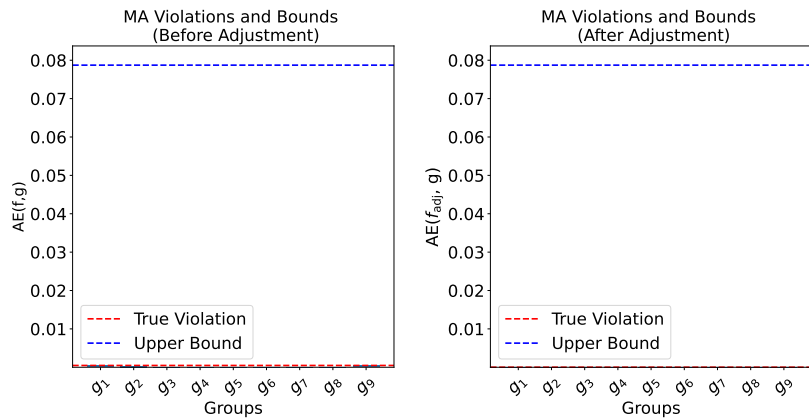


Figure B.7: $AE(f, g)$, $AE^{\max}(f, g)$ (dotted red line), and worst case violations (dotted blue line) of the original model f and adjusted model f_{adj} on ACSPubCov. Here, f is a Random Forest.

Figure B.8: Multiaccuracy results for ACSPubCov

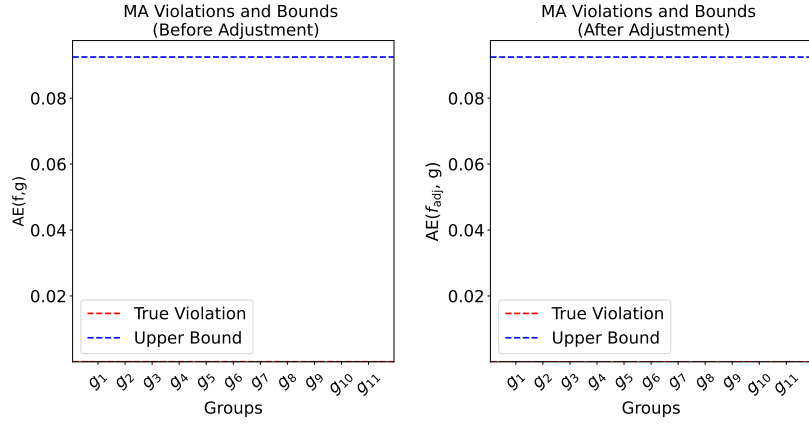


Figure B.9: $AE(f, g)$, $AE^{\max}(f, g)$ (dotted red line), and worst case violations (dotted blue line) of the original model f and adjusted model f_{adj} on CheXpert. Here, f is a logistic regression.

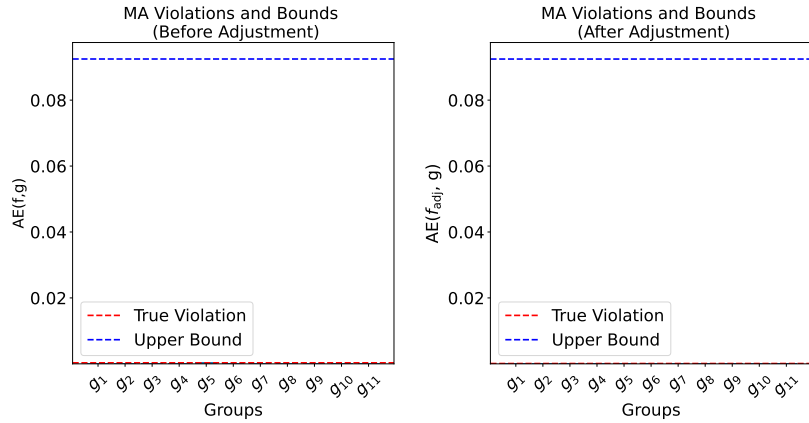


Figure B.10: $AE(f, g)$, $AE^{\max}(f, g)$ (dotted red line), and worst case violations (dotted blue line) of the original model f and adjusted model f_{adj} on CheXpert. Here, f is a decision tree.

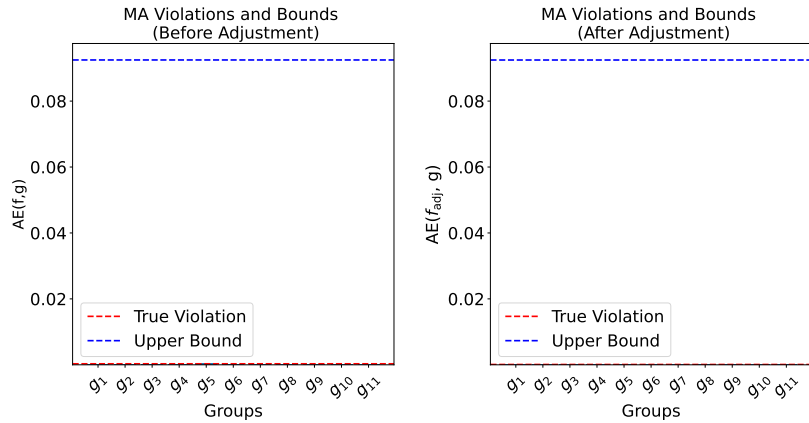


Figure B.11: $AE(f, g)$, $AE^{\max}(f, g)$ (dotted red line), and worst case violations (dotted blue line) of the original model f and adjusted model f_{adj} on CheXpert. Here, f is a DenseNet-121 model.

Figure B.12: Multiaccuracy results for CheXpert

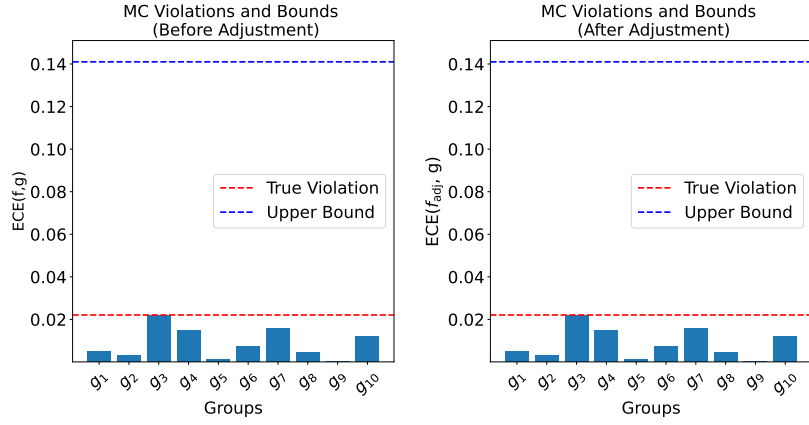


Figure B.13: ECE, ECE^{\max} (dotted red line), and worst case violations (dotted blue line) of the original model f and adjusted model f_{adj} on ACSIncome. Here, f is a logistic regression.

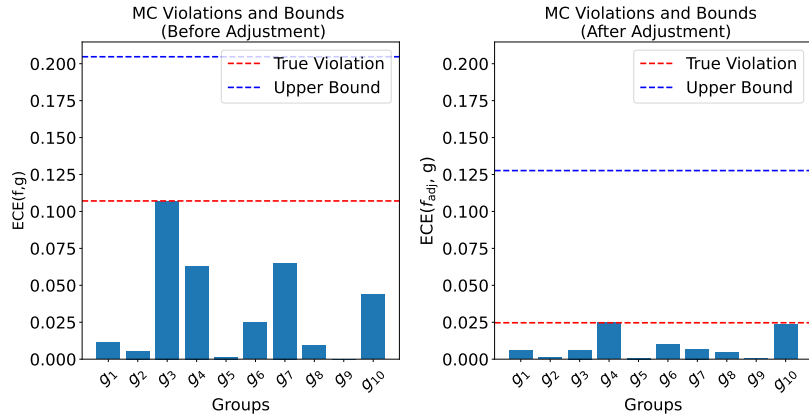


Figure B.14: ECE, ECE^{\max} (dotted red line), and worst case violations (dotted blue line) of the original model f and adjusted model f_{adj} on ACSIncome. Here, f is a decision tree.

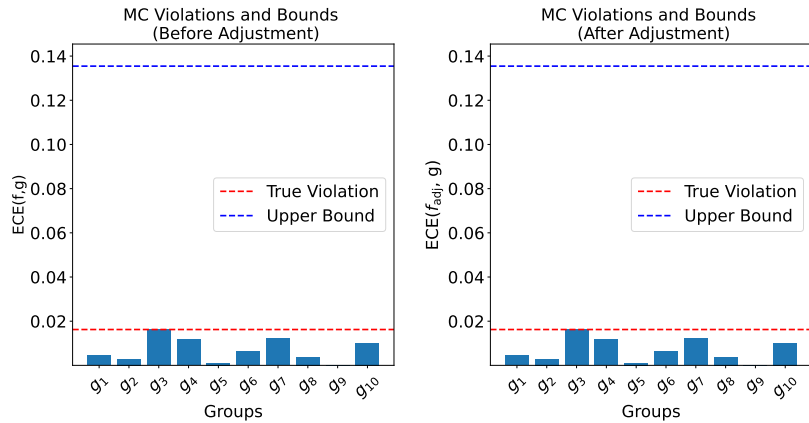


Figure B.15: ECE, ECE^{\max} (dotted red line), and worst case violations (dotted blue line) of the original model f and adjusted model f_{adj} on ACSIncome. Here, f is a Random Forest.

Figure B.16: Multicalibration results for ACSIncome

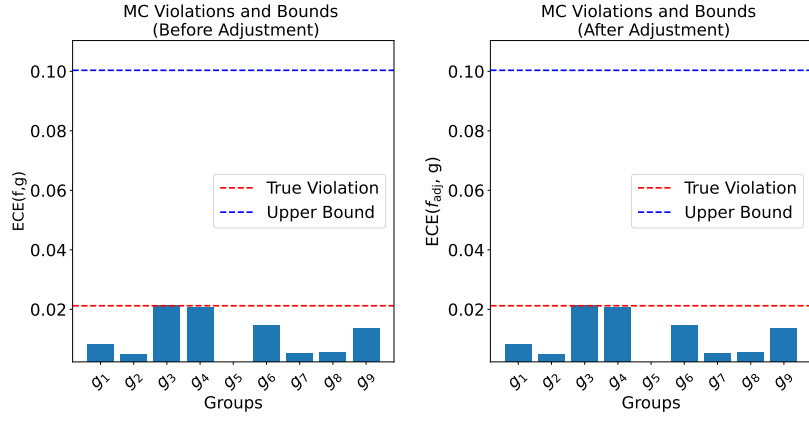


Figure B.17: ECE, ECE^{\max} (dotted red line), and worst case violations (dotted blue line) of the original model f and adjusted model f_{adj} on ACSPubCov. Here, f is a logistic regression.

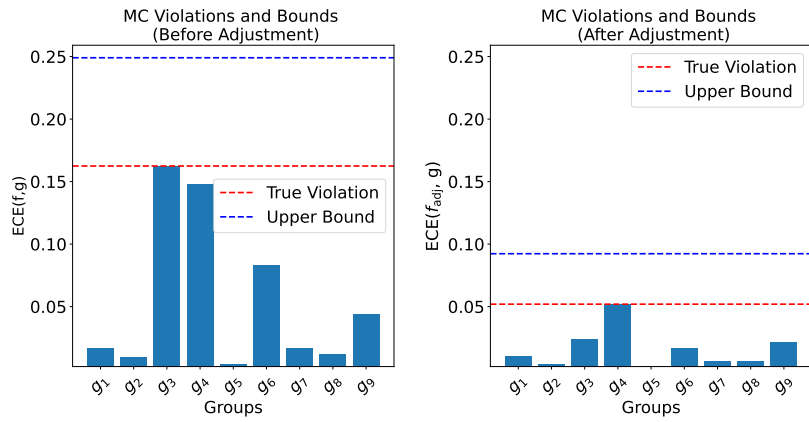


Figure B.18: ECE, ECE^{\max} (dotted red line), and worst case violations (dotted blue line) of the original model f and adjusted model f_{adj} on ACSPubCov. Here, f is a decision tree.

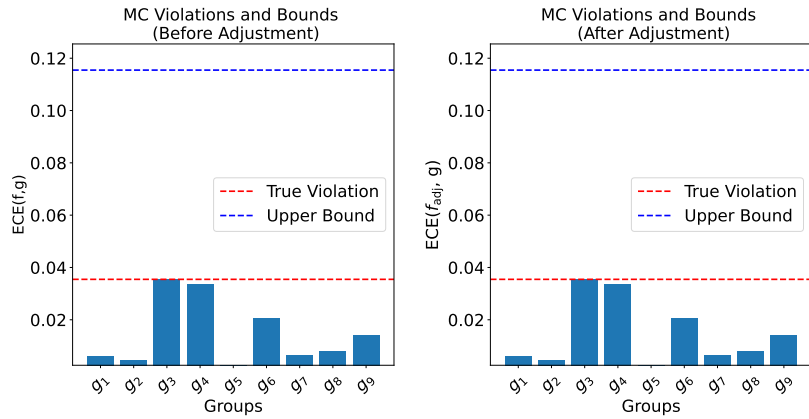


Figure B.19: ECE, ECE^{\max} (dotted red line), and worst case violations (dotted blue line) of the original model f and adjusted model f_{adj} on ACSPubCov. Here, f is a Random Forest.

Figure B.20: Multicalibration results for ACSPubCov

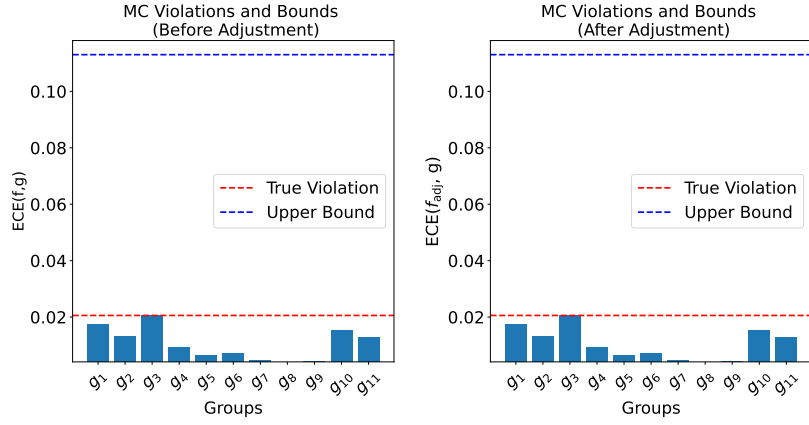


Figure B.21: ECE, ECE^{\max} (dotted red line), and worst case violations (dotted blue line) of the original model f and adjusted model f_{adj} on CheXpert. Here, f is a logistic regression.

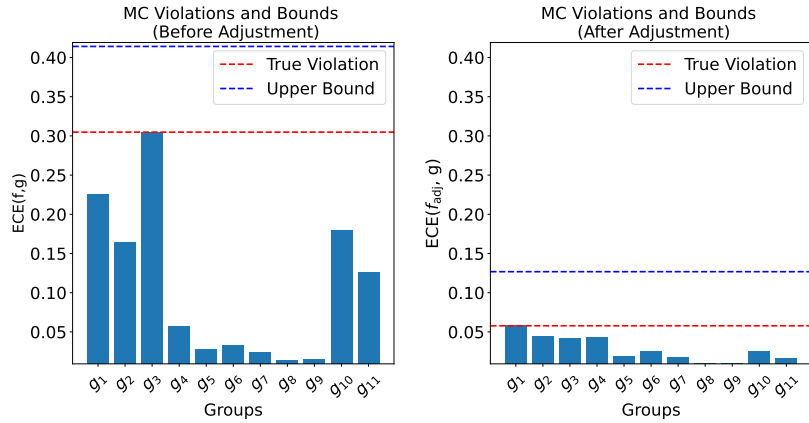


Figure B.22: ECE, ECE^{\max} (dotted red line), and worst case violations (dotted blue line) of the original model f and adjusted model f_{adj} on CheXpert. Here, f is a decision tree.

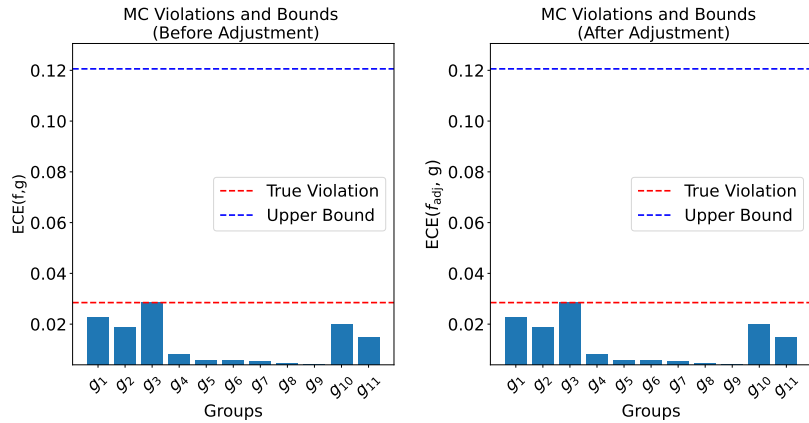


Figure B.23: ECE, ECE^{\max} (dotted red line), and worst case violations (dotted blue line) of the original model f and adjusted model f_{adj} on CheXpert. Here, f is a DenseNet-121 model.

Figure B.24: Multicalibration results for CheXpert